Stability Analysis of a Human Arm Interacting with a Force Augmenting Device

Sk Gadi, Antonio Osorio-Cordero, Rogelio Lozano, Ruben Garrido

Stability Analysis of a Human Arm Interacting with a Force Augmenting Device

Suresh K. Gadi · Antonio Osorio-Cordero · Rogelio Lozano · Ruben A. Garrido

S. K. Gadi (✉)
FIME, Universidad Autónoma de Coahuila, Torreón, Coah., Mexico 27276

A. Osorio · R. Lozano
UMI-LAFMIA, CINVESTAV-CNRS, Av. IPN 2508., Mexico City, 07360, Mexico

R. A. Garrido
Departamento de Control Automático, CINVESTAV, Av. IPN 2508., Mexico City, 07360, Mexico

Abstract

This paper presents a stability analysis of the interaction between a human and a linear mov-ing Force Augmenting Device (FAD). The analysis employs a mathematical model of the human arm, the FAD and their interaction. As a depart from past works, this article presents a stability analysis considering time-delays in the human model. A key ingredient in the analysis is the use of the Rekasius substitution for replacing the time-delay terms. It is proved that the human machine interaction is stable when the human model has no delays. When delays are considered in the human model, the analysis provides an upper bound for the time-delays preserving a stable interaction. Numerical simulations allow to assess the human-FAD interaction. An experiment is performed with a laboratory prototype, where a human operator lifts a load. It is observed that the human machine interaction is stable and the human opera-tor is able to move the load to a desired position by experiencing very little effort.

Delayed system · Force augmenting device · Stability analysis

1 Introduction

Recently, there has been a lot of interest in developing exoskeletons and force augmenting devices [1], i.e. mechanical systems that are worn by humans in such a way as to increase their force. There exist many possible applications for these devices; for instance, in industries where it is commonly required to move heavy loads. This task is mostly done by machines, which are usually controlled by humans who do not necessarily feel the force exerted on the load. This may lead to unsafe operations in confined spaces with obstacles. Exoskeletons and force augmenting devices (FAD) represent a possible solution to this problem [2]. Indeed a FAD amplifies the human strength and allows the operator handling heavy loads but still feeling the effort performed to move a load [3].

There are many papers in the literature dealing with human-machine interaction [4–10], however the stability of the proposed control algorithms has not been thoroughly studied. In order to study the stability of the human machine interaction we need to introduce a model for the human behaviour. There are several possible models for the human operator [11–15] and we have selected the model proposed in [12] because it takes into account the delays present in the human reflexes.

In this paper we present a simple controller for the FAD and a stability proof of its interaction with a human operator. We first study the stability of the interaction considering no delays in the human model. The closed loop system is of 4^{th} order and the proof of the stability is carried out using the Routh-Hurwitz stability criterion. Furthermore, we have also studied the stability considering delays in the human model. An upper bound for the delays has been found such that the stability is preserved. The human-FAD interaction is illustrated through numerical simulations.

The paper is organized as follows: The next section introduces a model of the FAD, a model of a human operator and the control algorithm proposed in [16, 17] for the FAD. This is followed by a section providing the stability proof for the system ignoring delays in the human model. Subsequently, the stability is studied considering that both delays in the human model are equal. In the next section a stability analysis is performed assuming that both delays in the human model are independent. Simulation and experimental results support the results obtained. Concluding remarks are given in the final section.

2 Nomenclature

θ_h	Human arm position
θ_{vd}	Virtual desired position
θ_v	Output of the spinal cords reflex action
τ_h	External torque acting on the human joint
B	Viscous friction in the human arm movement
d_1	Delay in the position reflex feedback
d_2	Delay in the velocity reflex feedback
E	Physical compliance of the human flesh
F	Total force exerted on the moving block
F_A	Force exerted by the motor on the moving block
F_e	Force exerted by the human on the moving block
F_h	Force exerted by the moving block on the human arm
g	Acceleration due to gravity
G_p	Control parameter of the spinal chord
G_v	Control parameter of the spinal chord
J	Human arm moment of inertia
K	Muscle stiffness
K_A	Force augmenting gain
K_d	Derivative gain
K_f	Viscous friction coefficient of FAD
K_p	Proportional gain
l_a	Human arm length
M	Mass of the moving block
s	Laplace transform complex variable
t	Time
W	Weight of the moving block
y_e	Position of the moving block
y_h	Human arm displacement at the end of the arm

3 Mathematical Model

The force augmenting device (FAD) considered in this paper is shown in Figs. 1a and b depicts its block diagram. This figure also shows the interaction between a human operator and the FAD. The FAD has a moving block of 24 kg connected to a ball-screw mechanism, and acts as the load to be lifted by the human operator. The ball-screw mechanism is driven by a DC servo motor. Force and position sensors are attached to the FAD to capture the force exerted by the human on the moving block and to measure its position respectively. The total force exerted on the moving block (F) can be decomposed as

$$F(t) = F_A(t) + F_e(t) - W \tag{1}$$

where F_A is the force exerted by the motor on the moving block, F_e is the force exerted by the human on the moving block, $W = Mg$ is the weight of the moving block, M is the mass of the moving block, g is the acceleration due to gravity and t is the time. Considering zero initial conditions, the dynamics of the moving block can be written as

$$\frac{y_e(s)}{F(s)} = \frac{1}{Ms^2 + K_f s} \tag{2}$$

where y_e is the position of the moving block, K_f is the viscous friction coefficient of the FAD and s is the Laplace transform complex variable.

The human model used for describing the human operator arm is based on a servo hypothesis proposed

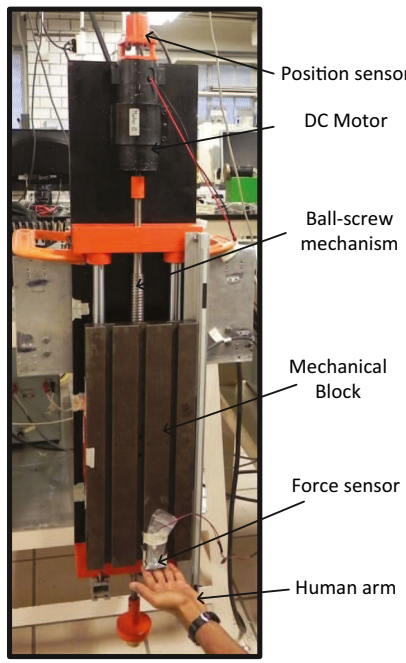

(a) Photo of a human operating a linear force augmenting device

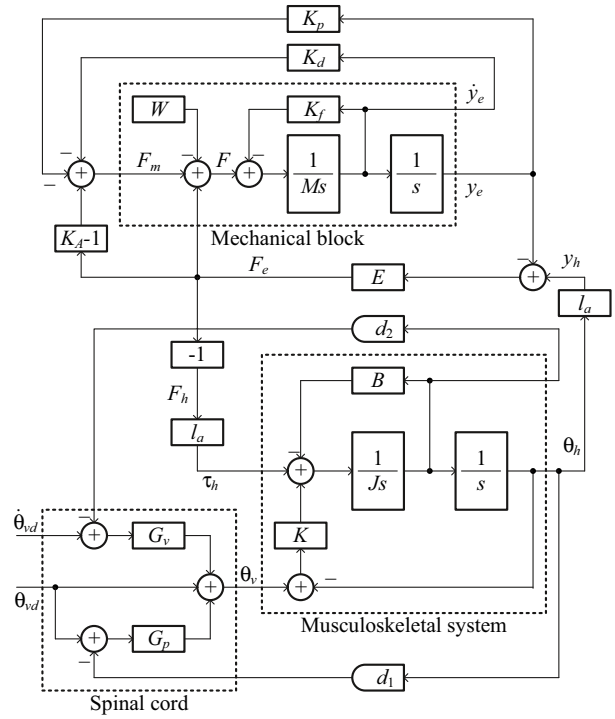

(b) Block diagram of the human-FAD interaction

Fig. 1 Human operating a force augmenting device

in [12], where the spinal cord actuates the muscles of the musculoskeletal system by processing the signals received from the brain, and the position and velocity feedback signals produced by the sensory organs of the musculoskeletal system. The position reached by the human arm is not exactly equal to the position commanded by the spinal cord due to the arm inertia, so the command given by the spinal cord to the musculoskeletal system is termed as the virtual position [12, 18]. The human brain generates a desired trajectory along which the arm must move; based on the desired trajectory the brain computes a signal and sends it to the spinal cord [13], which is the virtual desired position [12]. The musculoskeletal system is modeled as a second order linear transfer function.

The human arm can be modeled as a second order linear dynamic system [12, 13]. The torque produced at the joint is a function of the actual arm position and its velocity and the desired arm position and velocity. The authors of [12] presented a mathematical model for this torque. This model is an improved version based on the virtual trajectory control hypothesis. This model was experimentally validated by the authors of [12, 13] at various velocities. It is observed that this model is valid up to a velocity around 0.32 m s^1. Figure 1b shows the dynamics of the musculoskeletal system, which can by modeled as:

$$\tau_h(s) = J\ddot{\theta}_h(s) + B\dot{\theta}_h(s) + K(\theta_h(s) - \theta_v(s)) \quad (3)$$

where τ_h is the external torque acting on the human joint, θ_h is the human arm position, θ_v is the output of the spinal cords reflex action, J is the human arm moment of inertia, B is the viscous friction in the human arm movement and K is the muscle stiffness.

The term θ_v represents the virtual arm position. In a human being, the sensory feedback received by the spinal cord is delayed. This delay makes the stability issue challenging. The following equation represents the spinal cord reflex action:

$$\begin{aligned}\theta_v(s) = {} & \theta_{vd}(s) + G_p(\theta_{vd}(s) - \theta_h(s)e^{-sd_1}) \\ & + sG_v(\theta_{vd}(s) - \theta_h(s)e^{-sd_2})\end{aligned} \quad (4)$$

where θ_{vd} is the virtual desired position, G_p and G_v are the control parameters of the spinal chord, d_1 is

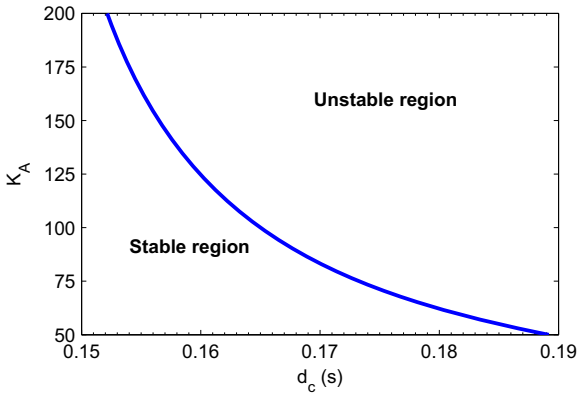

Fig. 2 Critical delay d_c at $50 \leq K_A \leq 200$ in equal delay case (i.e. $d_1 = D_2$)

the delay in the position reflex feedback and d_2 is the delay in the velocity reflex feedback.

The force exerted by the human arm F_e on the moving block can be expressed as

$$F_e(t) = -F_h(t) = (y_h(t) - y_e(t))E \tag{5}$$

$$y_h(t) = \theta_h(t) l_a \tag{6}$$

where F_h is the force exerted by the moving block on the human arm, E is the physical compliance of the human flesh, y_h is the human arm displacement at the end of the arm and l_a is human arm length.

The torque exerted by the moving block on the human arm, τ_h, can be given as

$$\tau_h(t) = F_h(t) l_a = (y_e(t) - y_h(t)) E l_a \tag{7}$$

The following control algorithm [16] is applied to the FAD:

$$F_A(t) = (K_A - 1)F_e(t) - K_d \dot{y}_e(t) - K_p y_e(t) \tag{8}$$

where K_A is the augmenting factor that amplifies the force exerted by the human operator, K_d is the derivative gain and K_p is the proportional gain.

Since the input terms W, y_{vd} and $s y_{vd}$ do not affect the stability, these terms can be neglected for the stability study. The characteristic equation for the closed loop system can be written as

$$P(s) = C_4 s^4 + C_3 s^3 + C_2 s^2 + C_1 s + C_0 \tag{9}$$

where

$$C_4 = JM \tag{10}$$

$$C_3 = M(B + G_v K e^{-sd_2}) + J(K_d + K_f) \tag{11}$$

$$C_2 = M(E l_a^2 + K(G_p e^{-sd_1} + 1)) + (K_d + K_f)(B + G_v K e^{-sd_2}) + J(K_p + E K_A) \tag{12}$$

$$C_1 = (B + G_v K e^{-sd_2})(K_p + E K_A) + (K_d + K_f)(E l_a^2 + K(G_p e^{-sd_1} + 1)) \tag{13}$$

$$C_0 = (K_p + E K_A)(E l_a^2 + K(G_p e^{-sd_1} + 1)) - E^2 K_A l_a^2 \tag{14}$$

In the following section we will study the stability of the above polynomial.

4 Stability Analysis When the Delays are Zero

Considering that $d_1 = d_2 = 0$, Eq. 9 can be rewritten as

$$P(s) = A_4 s^4 + A_3 s^3 + A_2 s^2 + A_1 s + A_0 \tag{15}$$

where

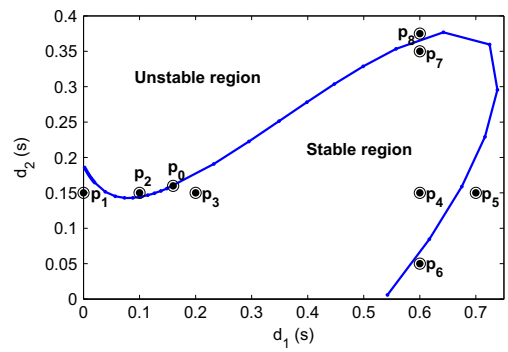

(a) critical delays for d_1 and d_2 at $K_A = 125$

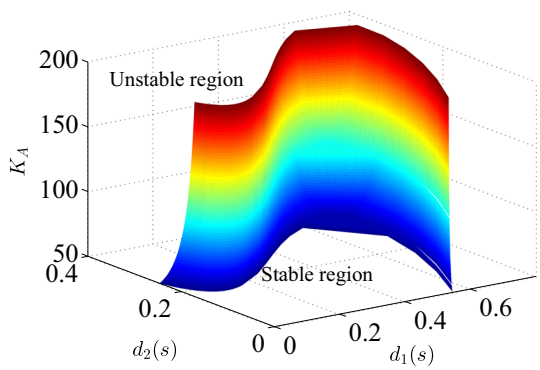

(b) critical delays for d_1 and d_2 at $50 \leq K_A \leq 200$

Fig. 3 Critical delay for d_1 and d_2

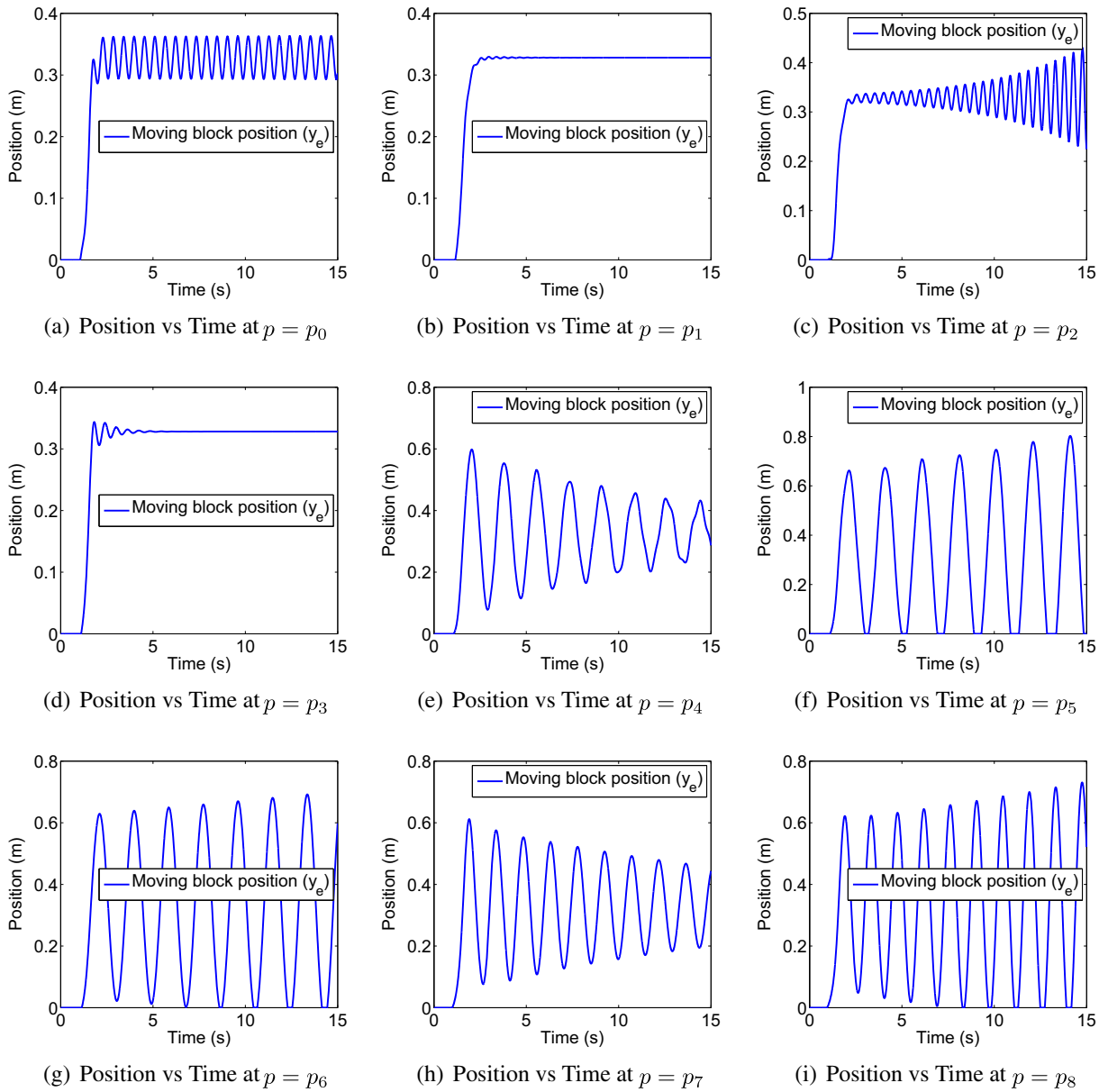

(a) Position vs Time at $p = p_0$ (b) Position vs Time at $p = p_1$ (c) Position vs Time at $p = p_2$

(d) Position vs Time at $p = p_3$ (e) Position vs Time at $p = p_4$ (f) Position vs Time at $p = p_5$

(g) Position vs Time at $p = p_6$ (h) Position vs Time at $p = p_7$ (i) Position vs Time at $p = p_8$

Fig. 4 Simulation results

$$A_4 = JM \tag{16}$$

$$A_3 = M(B + G_v K) + J(K_d + K_f) \tag{17}$$

$$A_2 = M(El_a^2 + K(G_p + 1)) + (K_d + K_f)(B + G_v K) + J(K_p + EK_A) \tag{18}$$

$$A_1 = (B + G_v K)(K_p + EK_A) + (K_d + K_f)(El_a^2 + K(G_p + 1)) \tag{19}$$

$$A_0 = EK_p l_a^2 + (G_p + 1)KK_p + E(G_p + 1)KK_A \tag{20}$$

As per the Routh-Hurwitz stability criterion, the closed loop system is stable if and only if

$$A_0 > 0;\ A_1 > 0;\ A_2 > 0;\ A_3 > 0;\ A_4 > 0;\ A_5 > 0 \tag{21}$$

$$b_1 := \left(A_3 A_2 - A_4 A_1\right)/A_3 > 0 \tag{22}$$

$$c_1 := \left(b_1 A_1 - A_3 A_0\right)/b_1 > 0 \tag{23}$$

The above conditions are indeed satisfied for all the positive values of the involved parameters [19]. In

the succeeding sections, a numerical example is introduced to study the stability considering the delays.

5 Stability Considering Identical Delays

Assume that both delays are the same, i.e. $d_1 = d_2 = d$. The substitution proposed by Rekasius is [20, 21]

$$e^{-sd} = \frac{1 - Ts}{1 + Ts} \qquad T \in \Re, \quad d \in \Re^{+} \tag{24}$$

which is defined when $s = j\omega$, $\omega \in \Re$. Unlike Pad approximation, this is an exact substitution. This substitution allows to replace the exponential transcendental term associated to the time-delay (i.e. e^{-sd}) by a rational expression of the variables s and T. It is observed that using this substitution leads to less conservative stability results than the approach employing Lyapunov-Krasovskii functionals [22]. We are using this fact to identify the exact point at which the system goes from stable to unstable. As opposed to other techniques, the values obtained with this approach are accurate. The relation between d , T and ω can be given as [20, 21]

$$\begin{aligned} d &= \frac{2}{\omega} \arctan(T\omega) + l\pi \\ l &= -\infty, \ldots -1, 0, 1, \ldots, \infty \end{aligned} \tag{25}$$

where for a fixed ω each T maps to infinitely many values of d. Substituting (24) into (9), we get

$$P(s) = B_5 s^5 + B_4 s^4 + B_3 s^3 + B_2 s^2 + B_1 s + B_0 \tag{26}$$

where

$$B_5 = JMT \tag{27}$$

$$B_4 = JM + BMT + J(K_d + K_f)T - G_v KMT \tag{28}$$

$$\begin{aligned} B_3 = {} & EMTl_a^2 + BM + J(K_d + K_f) \\ & + G_v KM + B(K_d + K_f)T + JK_pT + KMT \\ & + EJK_AT - G_v K(K_d + K_f)T \\ & - G_p KMT \end{aligned} \tag{29}$$

$$\begin{aligned} B_2 = {} & B(K_d + K_f) + JK_p + KM + EJK_A \\ & + G_v K(K_d + K_f) + G_p KM + BK_pT \\ & + K(K_d + K_f)T + EMl_a^2 \\ & + E(K_d + K_f)Tl_a^2 + BEK_AT \\ & - G_p K(K_d + K_f)T \\ & - G_v KK_pT - EG_v KK_AT \end{aligned} \tag{30}$$

$$\begin{aligned} B_1 = {} & BK_p + K(K_d + K_f) + BEK_A \\ & + G_p K(K_d + K_f) + G_v KK_p + KK_pT \\ & + E(K_d + K_f)l_a^2 \\ & + EK_pTl_a^2 + EG_v KK_A + EKK_AT \\ & - G_p KK_pT - EG_p KK_AT \end{aligned} \tag{31}$$

$$B_0 = EK_pl_a^2 + KK_p + EKK_A + G_p KK_p EG_p KK_A \tag{32}$$

The estimated values for the laboratory setup shown in Fig. 1a are $M = 23.4$ kg and $K_f = 0\,\mathrm{N\,m^{-1}}$. The authors in [12] use the following parameters for a human arm: $J = 0.1\,\mathrm{N\,m\,rad^{-1}\,s^{-1}}$, $B = 0.89\,\mathrm{N\,m\,rad^{-1}\,s^{-1}}$, $K = 4\,\mathrm{N\,m\,rad^{-1}}$, $G_p = 2$ and $G_v = 0.3$ s. The value $E = 920\,\mathrm{N\,m\,rad^{-1}}$ for human

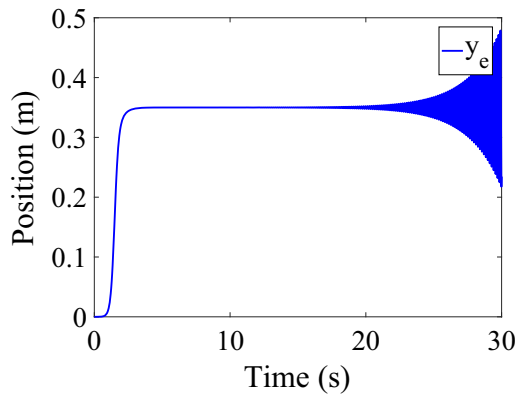

(a) Simulation results with $K_A = 100 \times 10^3$, $G_p = 2$ and $G_v = 1.11$

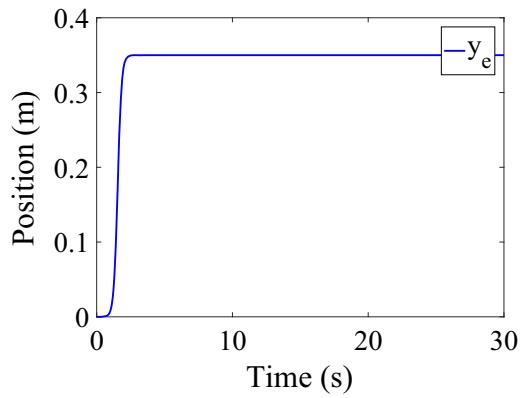

(b) Simulation results with $K_A = 100 \times 10^3$, $G_p = 2$ and $G_v = 0.3$

Fig. 5 Simulation results showing the effect of G_v in the stability of the human FAD interaction

flesh is given in [23]. Taking $l_a = 0.35$ m and the control parameters $K_A = 125$, $K_d = 65\,\mathrm{kg\,s^{-1}}$ and $K_p = 45\,\mathrm{kg\,s^{-2}}$. Substituting these values in $P(s)$, Eq. 26 is rewritten as

$$\begin{aligned} P(s) = {} & 2.3 \times 10^5 T s^5 \\ & + (2.3 \times 10^5 - 7.5 \times 10^4 T) s^4 \\ & + (1.4 \times 10^9 T + 5.5 \times 10^6) s^3 \\ & + (1.5 \times 10^9 - 2.9 \times 10^9 T) s^2 \\ & + (2.5 \times 10^{10} - 4.6 \times 10^{10} T) s \\ & + 1.4 \times 10^{11} \end{aligned} \tag{33}$$

Since the system is stable when the delays are zero, all the poles are in the left hand side of the complex plane. New poles are introduced from the left hand side of the complex plane as a consequence of the presence of delays [24]. The position of the poles in the complex plane as a function of the delay is continuous [24, 25]. As the delays increase, the poles move towards the right hand side of the plane and finally cross the $j\omega$ axis. The substitution (24) is valid at the moment when the poles are on the imaginary axis just before crossing it.

A Routh array can be constructed for Eq. 33 as

s^5	$2.3 \times 10^5 T$	$(140.3T + 0.6) \times 10^6$	B_{53}
s^4	$(2.3 - 0.8T) \times 10^5$	$(1.5 - 2.9T) \times 10^9$	B_{43}
s^3	B_{31}	B_{32}	0
s^2	B_{21}	1.4×10^{11}	0
s^1	B_{11}	0	0
s^0	1.4×10^{11}	0	0

where

$$\begin{aligned} B_{53} &= (2.5 - 4.6T) \times 10^{10} \\ B_{43} &= 1.4 \times 10^{11} \\ B_{31} &= 1 \times 10^8 \left(563.5T^2 - 12.8T + 1.3\right) \Big/ \left(23.4 - 7.5T\right) \\ B_{32} &= 5 \times 10^{10} \left(6.8T^2 - 89.9T + 11.6\right) \Big/ \left(23.4 - 7.5T\right) \\ B_{21} &= -1 \times 10^8 \left(16113.9T^3 - 8528.6T^2 + 114.2T - 5.3\right) \Big/ \left(563.5T^2 - 12.8T + 1.3\right) \\ B_{11} &= -1 \times 10^{10} \left(14.7T^4 - 37.7T^3 + 4.5T^2 - 0.07T + 2416.6\right) \Big/ \left(16.1T^3 - 8.5T^2 + 0.1T - 0.005\right) \end{aligned}$$

As per the Routh-Hurwitz stability criterion, when the poles are on the imaginary axis, a row of the Routh array becomes zero and its previous row is called the auxiliary polynomial. The auxiliary polynomial gives the location of the poles on the imaginary axis. Solving $B_{11} = 0$ and considering only real values for T, the solution is $T = 2.44372$ or $T = 0.11131$. The auxiliary polynomial (P_A) is given by the next expression

$$P_A = B_{21} s^2 + 1.4 \times 10^{11} \tag{34}$$

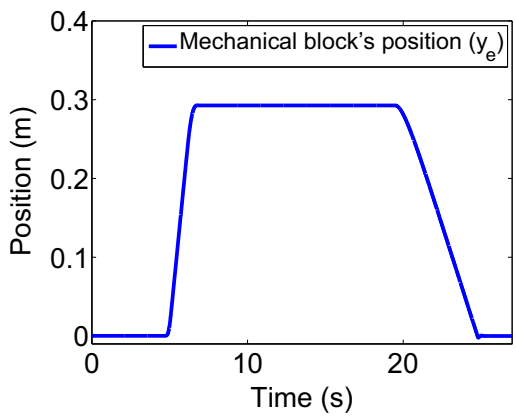

(a) Position vs time

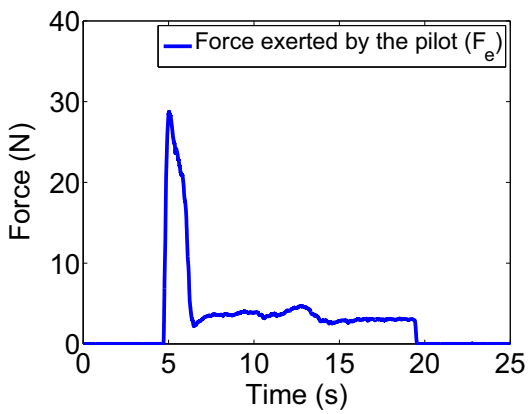

(b) Force vs time

Fig. 6 Experimental result

Solving (34) at $T = 2.44372$ and $T = 0.11131$, yields respectively $s = j\omega = \pm j(j5.0048)$ and $s = j\omega = \pm j11.1765$. Since $\omega \in \Re$, $T = 0.11131$, $\omega = 11.1765$ is the required value. As can be observed from Eq. 25, for given values of $\omega \in \Re$ and $T \in \Re$, an infinite number of time delays are generated for which a pair of poles are transferred from the left to the right complex plane. Equation 25 is used to obtain the following values:

$$\begin{aligned} d|_{l=0} &= 0.1599 \\ d|_{l=1} &= 3.3015 \\ d|_{l=-1} &= -2.9817 \end{aligned}$$

The smallest positive delay at which the poles cross the imaginary axis for the first time is called the critical delay (d_c). The critical delay for this system occurs for the values $l = 0$, $d = d_c = 0.1599$. Repeating the above calculations for the different values of K_A, we can obtain the critical delay corresponding to each value of K_A. Figure 2 shows the change in the critical delay as a function of the augmenting factor K_A.

6 Stability Considering Independent Delays

In this section let us consider different delays d_1 and d_2. A Rekasius substitution similar to Eq. 24 for the two time-delays is

$$e^{-sd_1} = \frac{1 - T_1 s}{1 + T_1 s} \qquad T_1 \in \Re, \quad d_1 \in \Re^+ \tag{35}$$

$$e^{-sd_2} = \frac{1 - T_2 s}{1 + T_2 s} \qquad T_2 \in \Re, \quad d_2 \in \Re^+ \tag{36}$$

and the relation between T_1, ω_1, and d_1 and T_2, ω_2, and d_2 is given by

$$d_1 = \frac{2}{\omega} \arctan(T_1\omega) + l\pi \qquad l = -\infty, \ldots -1, 0, 1, \ldots, \infty \tag{37}$$

$$d_2 = \frac{2}{\omega} \arctan(T_2\omega) + l\pi \qquad l = -\infty, \ldots -1, 0, 1, \ldots, \infty \tag{38}$$

Substituting (35) and (36) into (9), we get a characteristic polynomial of order six. Using the values for the parameters B, E, G_p, G_v, J, K, K_A, K_d, K_f, K_p, l_a, M given in the previous section, the following polynomial is obtained.

$$\begin{aligned} P(s) = {} & T_1T_2s^6 + (T_1 + T_2 - 0.3T_1T_2)s^5 \\ & +(23.7T_1 - 0.3T_2 + 6 \times 10^3 T_1T_2 + 1)s^4 + (6 \times 10^3 T_1 \\ & +6 \times 10^3 T_2 - 1 \times 10^4 T_1T_2 + 23.7)s^3 \\ & +(1.1 \times 10^5 T_1 - 1.2 \times 10^4 T_2 \\ & -2 \times 10^5 T_1T_2 + 6.2 \times 10^3)s^2 \\ & +(6 \times 10^5 T_2 - 2 \times 10^5 T_1 + 1.1 \times 10^5)s \\ & +6 \times 10^5 \end{aligned} \tag{39}$$

Giving T_1 a numerical value in Eq. 39, results in $P(s)$ depending only on T_2, giving a similar situation to Eq. 33. The computation for solving T given in the previous section can be used to obtain T_2, therefore the critical delays corresponding to T_1 and T_2 can be computed using (37) and (38).

Varying T_1 in the region [0.001 10] and solving for T_2 critical delays for d_1 and d_2 are obtained, see Fig. 3a. Also, varying K_A from 50 to 200, results in Fig. 3b which shows the critical delays of d_1 and d_2 as a function of K_A.

7 Simulation Results

A simulation has been performed on the system shown in Fig. 1a using MATLAB Simulink. A Runge-Kutta solver of 4^{th} order with a step size of 1 ms is used for the numerical simulation. Simulation is performed with the system parameters given in the previous sections and K_A is taken as 125. Let $p = (d_1, d_2)$ be any point on Fig. 3a representing delays. Simulation is performed at $p_0 = (0.1599, 0.1599)$, $p_1 = (0, 0.15)$, $p_2 = (0.1, 0.15)$, $p_3 = (0.2, 0.15)$, $p_4 = (0.6, 0.15)$, $p_5 = (0.7, 0.15)$, $p_6 = (0.6, 0.05)$, $p_7 = (0.6, 0.35)$, $p_8 = (0.6, 0.375)$. The simulation results are shown in Fig. 4.

Another simulation was performed to simulate the interaction between the human and the FAD at a high value of the force augmenting factor i.e. $K_A = 100 \times 10^3$, and considering $d_1 = d = 2 = 40$ ms. It has been observed from the simulations that the interaction is unstable for the values $G_p = 2$ and $G_v = 1.11$. However, it is observed that the interaction goes from the unstable region to the stable region just by changing the values of the constants internal to the human body, i.e. changing the value of G_v to 0.3. These results are shown in Fig. 5. Hence, through

the simulations, it is also possible to verify that the human's learning capability helps stabilizing the interaction.

8 Experimental Results

The prototype designed at the laboratory uses a computer with Windows XP operating system, which runs MATLAB-SIMULINK along with the WinCon software. This setup allows performing a real time experiment with the FAD. We have used a sampling time of 1 ms. The control parameters used for the experiments are $K_A = 125$, $K_d = 65\,\mathrm{kg\,s^{-1}}$ and $K_p = 45\,\mathrm{kg\,s^{-2}}$. Figure 6a and b show the experimental results. It can be noted from Fig. 6b that the human operator is experiencing a load of $\approx 2\,\mathrm{N} \approx 204$ g while lifting a mass of 24 kg.

The prototype at our laboratory remains stable for very high values of the gains. We have tried to reach the instability region by increasing the value of K_A but we have not succeeded to render it unstable. The following reasons may be a possible explanation for this behavior.

1. The delays in the human subject's reflex path are very small as compared to the critical delays of the system.
2. The torque produced by the electric motor driving the ball-screw mechanism saturates for high values of K_A, and such a non-linearity stabilizes the system.

9 Conclusion

In this paper we have analysed the stability of the interaction of a human and a FAD. We have considered a general human operator model proposed in [12]. We have proved the stability in the case of zero delays using the Routh-Hurwitz criterion. When the human model includes time-delays, we have also found an upper bound for the delays such that the stability is preserved.

It should be pointed out that the actual delays presented by any healthy human being are about four times smaller than the upper bound found for the delays in this study, beyond which instability will occur in the system. For this reason from a practical point of view, it can be considered that the scheme presented is robust enough to delays.

The numerical simulations presented show that if the delays are maintained below the upper bound found, the system is stable.

A real time experiment was conducted in a prototype. It was observed that the human machine interaction is stable and it is also observed that the damping introduced is sufficient enough to maintain the system without any oscillation. It is also observed that the operator is actually exerting a small fraction of the total force needed to lift the weight.

In this paper the stiffness and the viscosity parameters of the human arm have been considered constant. The stability analysis proves that the closed loop will remain stable for any positive values of these two coefficients. In the future we aim at improving the performance of the control strategy in the presence of variations of the stiffness and the viscosity parameters which may occur when changing the user.

Acknowledgments Work carried out in the UMI LAFMIA at CINVESTAV, Mexico in the framework of the Labex MS2T, funded by the French Government, through the National Agency for Research (Reference ANR-11-IDEX-0004-02). The authors would like to thank Gerardo Castro, and Jess Meza, for their help in implementing the electrical setup and Roberto Lagunes for his help in building the mechanical setup. Also, the authors are thankful to the reviewers for their valuable suggestions to improve the paper.

References

1. Guizzo, E., Goldstein, H.: The rise of the body bots [robotic exoskeletons]. IEEE Spectrum. **42**(10), 50–56 (2005)
2. Kim, W., Lee, S., Lee, H., Yu, S., Han, J., Han, C.: Development of the heavy load transferring task oriented exoskeleton adapted by lower extremity using qausi-active joints. In: ICCAS-SICE, 2009, pp. 1353–1358. IEEE (2009)
3. Snyder, T.J., Kazerooni, H.: A novel material handling system. In: 1996 IEEE International Conference on Robotics and Automation, 1996. Proceedings., vol. 2, pp. 1147–1152. IEEE (1996)
4. Specialty Materials Handling Products Operation. Hardiman 1 prototype project. Technical report, General Electric Company, Schenectady, New York 12305, December 1969
5. Kazerooni, H.: Human machine interaction via the transfer of power and information signals. In: ASME Winter Annual Meeting (1988)
6. Kazerooni, H.: Human-robot interaction via the transfer of power and information signals. IEEE Trans. Syst. Man Cybern. **20**(2), 450–463 (1990)
7. Lee, S., Sankai, Y.: Power assist control for leg with hal-3 based on virtual torque and impedance adjustment. In: 2002 IEEE International Conference on Systems, Man and Cybernetics, vol. 4, pp. 6–pp. IEEE (2002)

8. Yamamoto, K., Hyodo, K., Ishii, M., Matsuo, T.: Development of power assisting suit for assisting nurse labor. JSME Int. J. Series C **45**(3), 703–711 (2002)
9. Kazerooni, H.: The Berkeley lower extremity exoskeleton. In: Field and Service Robotics, pp. 9–15. Springer (2006)
10. Kong, K., Tomizuka, M.: Control of exoskeletons inspired by fictitious gain in human model. IEEE/ASME Trans. Mechatron. **14**(6), 689–698 (2009)
11. Merton, P.A.: Speculations on the servo-control of movement. In: Ciba Foundation Symposium-The Spinal Cord, pp. 247–260. Wiley Online Library (1953)
12. McIntyre, J., Bizzi, E.: Servo hypotheses for the biological control of movement. J. Motor Behav. **25**(3), 193–202 (1993)
13. Schweighofer, N., Arbib, M.A., Kawato, M.: Role of the cerebellum in reaching movements in humans. i. distributed inverse dynamics control. Eur. J. Neurosci. **10**(1), 86–94 (1998)
14. Schweighofer, N., Spoelstra, J., Arbib, M.A., Kawato, M.: Role of the cerebellum in reaching movements in humans. ii. a neural model of the intermediate cerebellum. Eur. J. Neurosci. **10**(1), 95–105 (1998)
15. Oshima, T., Fujikawa, T., Kameyama, O., Kumamoto, M.: Robotic analyses of output force distribution developed by human limbs. In: 9th IEEE International Workshop on Robot and Human Interactive Communication, 2000. RO-MAN 2000. Proceedings, pp. 229–234. IEEE (2000)
16. Gadi, S.K., Lozano, R., Garrido, R., Osorio, A.: Stability analysis and experiments for a force augmenting device. In: 9th International Conference on Electrical Engineering, Computing Science and Automatic Control (CCE), 2012, pp. 1–6 (2012)
17. Gadi, S.K., Garrido, R.A., Lozano, R., Osorio, A.: Stability analysis for a force augmenting device considering delays in the human model. In: ASME 2013 International Mechanical Engineering Congress and Exposition, pages V012T13A067–V012T13A067. American Society of Mechanical Engineers (2013)
18. Latash, M.L., Gottlieb, G.L.: Reconstruction of shifting elbow joint compliant characteristics during fast and slow movements. Neuroscience **43**(2–3), 697–712 (1991)
19. Gadi, S.K.: Modelado y control de un dispositivo de aumento de fuerza. PhD thesis, Centro de Investigación y de Estudios Avanzados del Instituto Politécnico Nacional, 5 (2014)
20. Olgac, N., Sipahi, R.: The direct method for stability analysis of time delayed LTI systems. In: American Control Conference, 2003. Proceedings of the 2003, vol. 1, pp. 869–874. IEEE (2003)
21. Rekasius, Z.V.: A stability test for systems with delays. In: Proceedings of the Joint Automatic Control Conference, San Francisco, CA, paper TP9-A (1980)
22. Ebenbauer, C., Allgöwer, F.: Stability analysis for time-delay systems using rekasius's substitution and sum of squares. In: 45th IEEE Conference on Decision and Control, pp. 5376–5381. IEEE (2006)
23. Pataky, T.C., Latash, M.L., Zatsiorsky, V.M.: Viscoelastic response of the finger pad to incremental tangential displacements. J. Biomech. **38**(7), 1441–1449 (2005)
24. Michiels, W., Niculescu, S.I.: Stability and Stabilization of Time-Delay Systems: An Eigenvalue-Based Approach. Advances in Design and Control. Society for Industrial and Applied Mathematics (2008)
25. Neimark, J.: D-subdivisions and spaces of quasipolynomials. Prikladnaya Matematika i Mekhanika **13**, 349–380 (1949)